Characterization and mechanical removal of metallic aluminum (Al) embedded in weathered municipal solid waste incineration (MSWI) bottom ash for application as supplementary cementitious material

Chen, Boyu; Chen, Jiayi; de Mendonça Filho, Fernando França; Sun, Yubo; van Zijl, Marc Brito; Copuroglu, Oguzhan; Ye, Guang

DOI
10.1016/j.wasman.2024.01.031

Publication date
2024

Document Version
Final published version

Published in
Waste Management

Citation (APA)
Chen, B., Chen, J., de Mendonça Filho, F. F., Sun, Y., van Zijl, M. B., Copuroglu, O., & Ye, G. (2024). Characterization and mechanical removal of metallic aluminum (Al) embedded in weathered municipal solid waste incineration (MSWI) bottom ash for application as supplementary cementitious material. *Waste Management*, *176*, 128-139. https://doi.org/10.1016/j.wasman.2024.01.031

Waste Management 176 (2024) 128–139

Contents lists available at ScienceDirect

Waste Management

journal homepage: www.elsevier.com/locate/wasman

Research Paper

Characterization and mechanical removal of metallic aluminum (Al) embedded in weathered municipal solid waste incineration (MSWI) bottom ash for application as supplementary cementitious material

Boyu Chen [a,*], Jiayi Chen [a], Fernando França de Mendonça Filho [a], Yubo Sun [b], Marc Brito van Zijl [c], Oguzhan Copuroglu [a], Guang Ye [a,b]

[a] Microlab, Section Materials and Environment, Faculty of Civil Engineering and Geosciences, Delft University of Technology, Stevinweg 1, 2628 CN Delft, The Netherlands
[b] Magnel-Vandepitte Laboratory, Department of Structural Engineering and Building Materials, Ghent University, 9052 Ghent, Belgium
[c] Mineralz (part of Renewi), Van Hilststraat 7, 5145 RK Waalwijk, The Netherlands

ARTICLE INFO

Keywords:
Weathering
Municipal solid waste incineration (MSWI) bottom ash
Metallic aluminum (Al) distribution
Mechanical treatments
Supplementary cementitious material (SCM)

ABSTRACT

Municipal solid waste incineration (MSWI) bottom ash, due to its high mineral content, presents great potential as supplementary cementitious material (SCM). Weathering, also known as aging, is a treatment process commonly employed in waste management to minimize the risk of heavy metal leaching from MSWI bottom ash. Using weathered MSWI bottom ash to produce blended cement pastes is considered as a high-value-added and sustainable waste disposal solution. However, a critical challenge arises from the metallic aluminum (Al) in weathered MSWI bottom ash, which is known to induce detrimental effects such as volume expansion and strength loss of blended cement pastes. While most metallic Al in weathered MSWI bottom ash can be removed with eddy current separators in metal recovery plants, the residual metallic Al, owing to its small particle size, cannot be removed with the same technique. This study is dedicated to addressing this issue. An in-depth analysis was conducted on residual metallic Al embedded in weathered MSWI bottom ash particles, aiming to guide the removal of this metal. This analysis revealed that mechanical removal was the most suitable method for extracting metallic Al. The specific processes and mechanisms underlying this method were elucidated. After reducing metallic Al content in weathered MSWI bottom ash by 77 %, a significant improvement in the quality of blended cement pastes was observed. This work contributes to the broader adoption of mechanical treatments for removing residual metallic Al from weathered MSWI bottom ash and facilitates the application of treated ash as SCM.

1. Introduction

The global waste-to-energy market, valued at USD 33 billion in 2020, is expected to grow at an annual rate of 7.4 %, reaching USD 55 billion in 2027 (Grand View Research, 2019). With the wide application of waste incineration techniques, the amount of municipal solid waste incineration (MSWI) residue to be disposed of is increasing rapidly in China, India, European Union countries, and the United States (Eurostat, 2023; IRENA, 2022; NBS, 2022; US EPA, 2022). The ash collected at the bottom of the combustion furnace, commonly referred to as MSWI bottom ash, accounts for 80–90 wt% of the total incineration residue (Chimenos et al., 1999; Lin and Lin, 2006). This significant proportion underscores the importance of recycling MSWI bottom ash to mitigate the environmental issues associated with its landfill disposal.

In recent years, the recycling of MSWI bottom ash as supplementary cementitious material (SCM) has attracted increasing attention (Chen et al., 2023a). Replacing cement clinker with MSWI bottom ash can save natural resources and reduce the carbon footprint associated with clinker manufacturing (Chen, 2023; Margallo et al., 2014). This action also provides a solution to future shortages of currently most used supplementary cementitious materials (including blast furnace slag and coal fly ash) (IEA, 2009). There are mainly two types of MSWI bottom

* Corresponding author.
E-mail addresses: B.Chen-4@tudelft.nl (B. Chen), J.Chen-2@tudelft.nl (J. Chen), F.Filho@tudelft.nl (F.F. de Mendonça Filho), Yubo.Sun@UGent.be (Y. Sun), Marc.Brito.van.Zijl@mineralz.com (M.B. van Zijl), O.Copuroglu@tudelft.nl (O. Copuroglu), G.Ye@tudelft.nl (G. Ye).

https://doi.org/10.1016/j.wasman.2024.01.031
Received 18 October 2023; Received in revised form 14 January 2024; Accepted 18 January 2024
Available online 27 January 2024

ash: fresh MSWI bottom ash and weathered MSWI bottom ash (Chen et al., 2023a). Fresh MSWI bottom ash is collected right after being discharged from the combustion chamber. Weathered MSWI bottom ash is produced after subjecting fresh MSWI bottom ash to the weathering process. This treatment is crucial for stabilizing the heavy metals and soluble salts present in the ash (Chen et al., 2023a; Chimenos et al., 2000). Compared with fresh MSWI bottom ash, weathered MSWI bottom ash has much lower leaching potential and is more suitable to be used as an ingredient for construction materials (Chen et al., 2023a).

The presence of aluminum (Al) is one of the main factors inhibiting the wide application of MSWI bottom ash in the construction industry (Chen et al., 2023a). When used as SCM, MSWI bottom ash is always ground into powder, exposing the metallic Al that would otherwise be covered by the mineral phases. This exposed metallic Al will react under the alkaline condition in blended cement system and release hydrogen gas, resulting in significant volume expansion and strength decrease (Tang et al., 2016). The MSWI bottom ash blended cement concrete with porous structures exhibited low strength (Kim et al., 2016) and poor resistance to chloride diffusion and carbonation (Simões et al., 2021). For the application of SCM, it is recommended to reduce the metallic Al content in MSWI bottom ash to improve the strength and long-term durability of MSWI bottom ash blended cement products (Alderete et al., 2021; Bertolini et al., 2004; Carsana et al., 2016; Chen et al., 2023a; Joseph et al., 2020; Tang et al., 2016). It is important to note that the metal recovery process is usually applied to MSWI bottom ash to ensure that the ash used as construction material has a low metal content (Chen et al., 2023a). During this process, the majority of metallic Al in MSWI bottom ash can be extracted with eddy current separators (Chen et al., 2023a; de Vries, 2017; Šyc et al., 2020). The residual metallic Al cannot be removed by the same technique. This is because the efficiency of eddy current separators is reduced when dealing with small metallic Al particles, especially those smaller than 2 mm and covered with mineral phases (Bunge, 2016; Holm and Simon, 2017; Neuwahl et al., 2019).

Knowing the distribution of metallic Al in MSWI bottom ash can help in selecting a suitable method to reduce its metallic Al content. The distribution of metallic Al in weathered MSWI bottom ash particles differs from that in fresh MSWI bottom ash particles. During the weathering process, fresh MSWI bottom ash readily reacts with the oxygen, carbon dioxide, and water in the surroundings (Bunge, 2016; de Vries et al., 2009; Saffarzadeh et al., 2016, 2011; Speiser et al., 2000). As a result of weathering, part of the metallic Al embedded in fresh MSWI bottom ash is oxidized. A significant reduction in metallic aluminum content was detected after weathering (de Vries et al., 2009; Joseph et al., 2020). To the best of our knowledge, the distribution of metallic Al among different size fractions of weathered MSWI bottom ash particles has not been comprehensively studied yet. In previous research, only the metallic Al embedded in fresh MSWI bottom ash particles was studied (Saffarzadeh et al., 2016; Xuan and Poon, 2018).

Different methods have been proposed to deal with the residual metallic Al in MSWI bottom ash after the metal recovery process. These methods include mechanical treatments, chemical treatments (e.g., water treatment and NaOH solution treatment), and thermal treatments (Chen et al., 2023a). Mechanical treatments have advantages over chemical treatments and thermal treatments. Mechanical treatments usually consist of grinding and sieving. The purpose of grinding is to reduce the particle size of MSWI bottom ash. Due to size reduction, the homogeneity in the compositions of MSWI bottom ash is also increased after mechanical treatments. Metallic Al can be separated from MSWI bottom ash by sieving during mechanical treatments. Mechanical treatments are usually performed at room temperature, and no wastewater is discharged during this process. In comparison, water treatment is used together with thermal treatments to reduce the metallic Al content in MSWI bottom ash. The reason for integrating thermal treatments with water treatment is to accelerate the reaction between metallic Al and water and to evaporate the water added during the water treatment (Joseph et al., 2020). The residual alkalis in NaOH solution-treated MSWI bottom ash need to be removed for the application as SCM, leading to the discharge of wastewater (Chen et al., 2019; Liu et al., 2018). Thermal treatments can be more expensive than mechanical treatments. During thermal treatments, the heating temperature needs to reach 1000 °C to oxidize more than 90 wt% of the metallic Al in MSWI bottom ash (Chen et al., 2020; Sun et al., 2019). Due to the agglomeration of particles, additional mechanical treatments are employed to reduce the particle size and make thermally treated MSWI bottom ash suitable for the application of SCM (Sun et al., 2019).

Although mechanical treatments have been used by previous researchers to remove metallic Al from MSWI bottom ash, there is no systematic guidance on the use of this method (Chen et al., 2023a). The parameter settings for mechanical treatments are usually determined by trial and error. Even at optimal parameter setting, some metallic Al remains in mechanically treated MSWI bottom ash (Chen et al., 2019; Joseph et al., 2020; Tang et al., 2016). This work aims to provide an in-depth understanding of the metallic Al embedded in weathered MSWI bottom ash particles and to develop knowledge that can be used to guide the mechanical removal of metallic Al from weathered MSWI bottom ash. This work consists of two parts:

Part 1 is to study the metallic Al in weathered MSWI bottom ash. The distribution of metallic Al among different size fractions of weathered MSWI bottom ash is measured. The particles that contain metallic Al are characterized to investigate the metallic Al embedded in weathered MSWI bottom ash particles.

In part 2, mechanical treatments are selected to remove metallic Al from weathered MSWI bottom ash according to the information obtained in part 1. The extent to which the metallic Al can be removed via mechanical treatments is discussed. The effectiveness of mechanical treatments in improving the strength of weathered MSWI bottom ash blended cement pastes is studied.

2. Materials and methods

2.1. Materials

The weathered MSWI bottom ash used in this work has a particle size below 1.6 mm (Fig. 1 (a)), which meets the maximum feed size requirements of the milling machine. To analyze the distribution of metallic Al across different size fractions, weathered MSWI bottom ash was sieved into five size groups: 0.5–1.6 mm, 0.25–0.5 mm, 0.125–0.25 mm, 0.063–0.125 mm, and <0.063 mm. The sieves were selected according to standards (NEN-EN 933-1, 2012; NEN-EN 933-2, 2020). The images of all these size fractions are illustrated in Fig. 1 (b), where the proportion of each size group in the MSWI bottom ash is also indicated. Details regarding the chemical and mineralogical compositions of these size groups are provided in Appendix A.

Our weathered MSWI bottom ash was obtained by crushing 4–11 mm MSWI bottom ash aggregates (see Fig. B1 in Appendix B) with Retsch® BB100. The crushing process was performed in a way similar to that employed by Van de Wouw (van de Wouw et al., 2020). The MSWI bottom ash aggregates were produced in a Dutch waste-to-energy plant. The plant-scale treatments of MSWI bottom ash aggregates followed the strategy described by Keulen et al. (Keulen et al., 2016), where the MSWI bottom ash was treated with dry separation, wet separation, and weathering. Most of the ferrous and non-ferrous metals were extracted during the dry separation process. The organic and inorganic leachable contaminants were removed in the wet separation process. The weathering process took around 3 months, and the goal was to immobilize heavy metals. After plant-scale treatments, the heavy metal leaching of MSWI bottom ash aggregates complied with the open (granular) application criteria of the Dutch Soil Quality Decree (Keulen et al., 2016).

Apart from weathered MSWI bottom ash, Portland cement (type I 52.5R, ENCI B.V.) and Class F coal fly ash were also used in this work. The Class F coal fly ash (FA) was provided by Vliegasunie B.V. and had

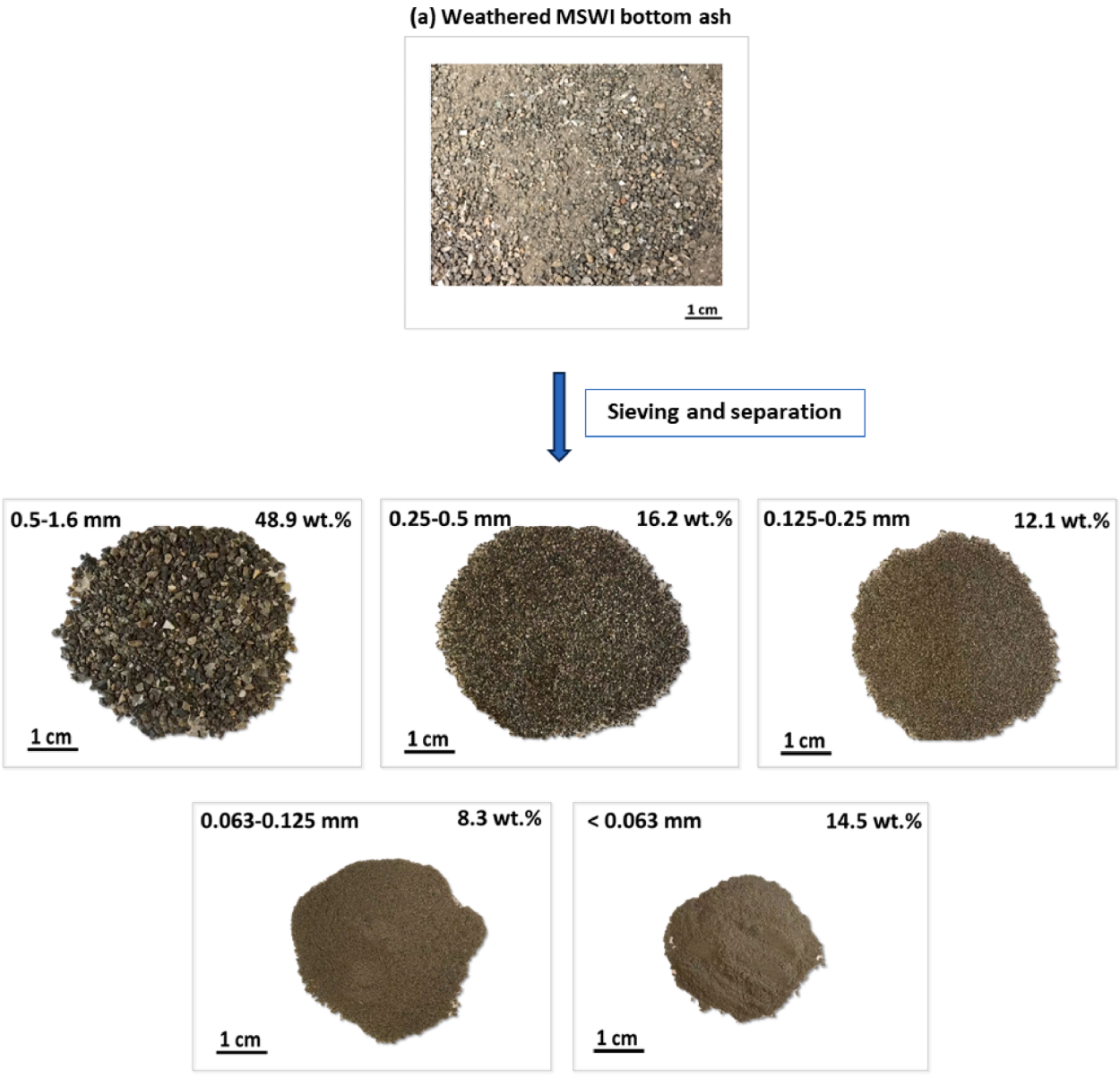

Fig. 1. Image of (a) weathered MSWI bottom ash; (b) different size fractions of weathered MSWI bottom ash.

chemical and mineralogical compositions the same as that used in our previous research (Chen et al., 2023b). The use of Class F coal fly ash as a reference for weathered MSWI bottom ash is due to their comparable pozzolanic reactivity (Chen et al., 2023a, 2023b).

2.2. Methods used to characterize metallic Al in weathered MSWI bottom ash

2.2.1. Metallic Al content measurement

The metallic Al content in weathered MSWI bottom ash and the metal scraps separated from weathered MSWI bottom ash is determined with the water displacement method (Qiao et al., 2008). Detailed information about this method can be found in Appendix B (see Fig. B2). It is worth noting that the water displacement method cannot distinguish the hydrogen gas (H_2 gas) released from the reaction of metallic Al and the reaction of metallic Zn. In our preliminary research, metallic Zn was hardly detected. A similar observation that the metallic Zn content was much less than metallic Al was reported in the literature for the MSWI bottom ash produced in the Netherlands (Muchova et al., 2009; Rem et al., 2004). Therefore, in the calculation, all the H_2 gas collected was attributed to the reaction of metallic Al, and the contribution of metallic Zn to the release of the H_2 gas was neglected.

2.2.2. Metallic Al identification by image analysis

The Energy Dispersive X-rays spectroscopy (EDS) combined with scanning electron microscopy (SEM) was used to measure the elemental distribution within weathered MSWI bottom ash particles and identify those containing metallic Al. The size fraction of 0.5–1.6 mm was chosen for this analysis because it had the highest metallic Al content. More explanations for this selection will be presented in Section 3.1.1. As for SEM sample preparation, several hundred randomly selected weathered MSWI bottom ash particles were mounted in epoxy resin (see Fig. B3 in Appendix B). The mold was a polyethylene bottle with a diameter of 35 mm. For the sake of avoiding metallic Al oxidation, mounted samples

were ground and polished to a flat surface using isopropanol in a N_2 - atmosphere glove box. Afterward, the polished samples were coated with a thin layer of carbon (around 10 nm) to improve their conductivity under a high vacuum. The samples were analyzed using FEI QUANTA FEG 650 ESEM. The accelerating voltage and working distance of the measurement were set as 15 kV and 10 mm, respectively.

The optimal microscope settings for microanalysis were determined with Monte Carlo simulation in WinCasino v2.51 software. In the microanalysis, the phases of interest were metallic Al (including alloys of Al) and the oxidized Al (Al_2O_3 and $Al(OH)_3$). Fig. B4 provides visual depictions of the lateral extent of the X-ray interaction volume of metallic Al, aluminum oxides (Al_2O_3), and aluminum hydroxides ($Al(OH)_3$) (see Appendix B). The pixel size of 2 μm was selected because it was close to the lateral dimension of the interaction volume of metallic Al. After elemental mapping, the spectral imaging (SI) data sets (atomic percentage) were acquired for the identification of metallic Al, aluminum oxide, and aluminum hydroxide in image analysis.

The process of image analysis used in this work is illustrated in Fig. B5 (see Appendix B). The first step was phase segmentation, which was carried out following Otsu's method (Otsu, 1979). The image thresholding was performed on the atomic ratio between oxygen and aluminum (O/Al) at each pixel location of the SEM images. The regions enriched with the phases, including metallic Al (Al), oxidized Al (Al-O), and Al alloy (e.g., Al-Fe or Al-Cu), were identified in the SEM images of MSWI bottom ash particles. For each segmented phase, their area percentage, average composition, and average O/Al ratio were calculated based on the information of corresponding pixels. In step two, the presence of Al_2O_3 and $Al(OH)_3$ in segmented oxidized Al phase was demonstrated by creating density plots. Each point in the density plots represented the atomic percentages of Al and O at each pixel in the region of the Al-O phase. The density plots were colored according to the number of points in each area.

2.3. Mechanical treatments of weathered MSWI bottom ash

In this work, weathered MSWI bottom ash was loaded in the planetary ball mill (Retsch® PM 100). According to the performance of the ball mill, the grinding speed was set between 200 and 350 rpm. The milling duration was controlled between 20 and 30 min. Grinding weathered MSWI bottom ash into powder reduced its particle size, as well as the heterogeneity in its composition. The metallic Al was removed by passing ground MSWI bottom ash (GBA) through the sieve of 0.063 mm. The substantial size difference between metallic Al and bottom ash particles allowed for the effective separation of this metal during the sieving process (see more details in Section 3.2.1). The MSWI bottom ash powder obtained after sieving is named mechanically treated MSWI bottom ash (MBA), as shown in Fig. 2.

2.4. Preparation and testing of weathered MSWI bottom ash blended cement pastes

As mentioned in the introduction part, the main purpose of reducing the metallic Al content in weathered MSWI bottom ash is to improve the strength of weathered MSWI bottom ash blended cement pastes. In this work, GBA and MBA were used to prepare blended cement pastes, respectively. The MBA was obtained after sieving out metallic Al from GBA and had much lower metallic Al content than GBA. The compressive strength of blended cement paste samples prepared with GBA and MBA was compared to examine the effectiveness of mechanical treatments on strength improvement.

The compressive strength of MBA blended cement paste (MBA-CEM) was also compared with that of Class F coal fly ash blended cement paste (FA-CEM) to assess whether MBA could be used as an alternative to FA. This is because the pozzolanic reactivity of weathered MSWI bottom ash is found to be similar to that of Class F coal fly ash (Chen et al., 2023a, 2023b). Since the percentage of coal fly ash added as SCM in concretes usually ranges from 15 wt% to 35 wt% (Yao et al., 2015), the percentage of Portland cement replaced by GBA, MBA or FA in blended cement is chosen to be 25 wt%, which is an intermediate value. Another reason for this choice is that in most previous cases, the replacement level of MSWI bottom ash did not exceed 30 wt% to prevent excessive leaching of contaminants from MSWI bottom ash blended cement pastes, mortars, and concretes to the environment (Li et al., 2012; Lin et al., 2008; Lin and Lin, 2006; Lo et al., 2020; Loginova et al., 2021; Tang et al., 2016; Yang et al., 2018b, 2018a).

In addition to blended cement paste samples, Portland cement paste samples (CEM) were also prepared as the reference group. A water-to-binder ratio of 0.5 was used for sample preparation to mimic the situation in concrete. When preparing plain cement pastes, Portland cement was directly mixed with water. For the preparation of blended cement paste samples, the SCM was first blended with Portland cement. Afterward, the dry powder blends were directly mixed with water to prepare fresh paste mixtures.

All the fresh pastes were mixed for 4 min with a high-shear mixer (model IKA® T 50 ULTRA-TURRAX®) and then cast in the mold with the dimension of 20 × 20 × 20 mm^3. The cement paste specimens were first cured at room temperature for 24 h. After demolding, the specimens were sealed with cling film and cured in a fog room (20 °C, 99 % relative humidity) until 28 days. The compressive strength of cubic paste samples was measured following the test procedure described in standard (NEN-EN 196-1, 2016).

3. Results and discussion

3.1. Metallic Al embedded in weathered MSWI bottom ash

It is essential to comprehend the distribution and characteristics of metallic Al embedded in weathered MSWI bottom ash. These insights are fundamental to the subsequent discussions on selecting the most optimal removal methods.

3.1.1. Distribution of metallic Al among different size fractions

The distribution of metallic Al was studied by measuring the metallic Al content in each size fraction and finding the size fraction with the highest percentage of metallic Al in weathered MSWI bottom ash. As shown in Fig. 3 (a), the metallic Al content decreases from 0.71 wt% in 0.5–1.6 mm size fraction to almost zero in the size fraction below 0.063 mm. Fig. 3 (b) indicates that 73 % of the metallic Al detected in weathered MSWI bottom ash is embedded in particles of 0.5–1.6 mm. The particles larger than 0.25 mm contain around 90 % of the metallic Al in weathered MSWI bottom ash. Considering the distribution of metallic Al among different size fractions, removing metallic Al from the coarse particles (>0.25 mm) is of high importance for the metallic Al content reduction in weathered MSWI bottom ash.

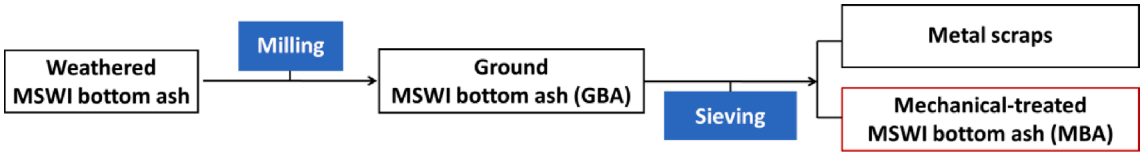

Fig. 2. Flow chart of mechanical treatments.

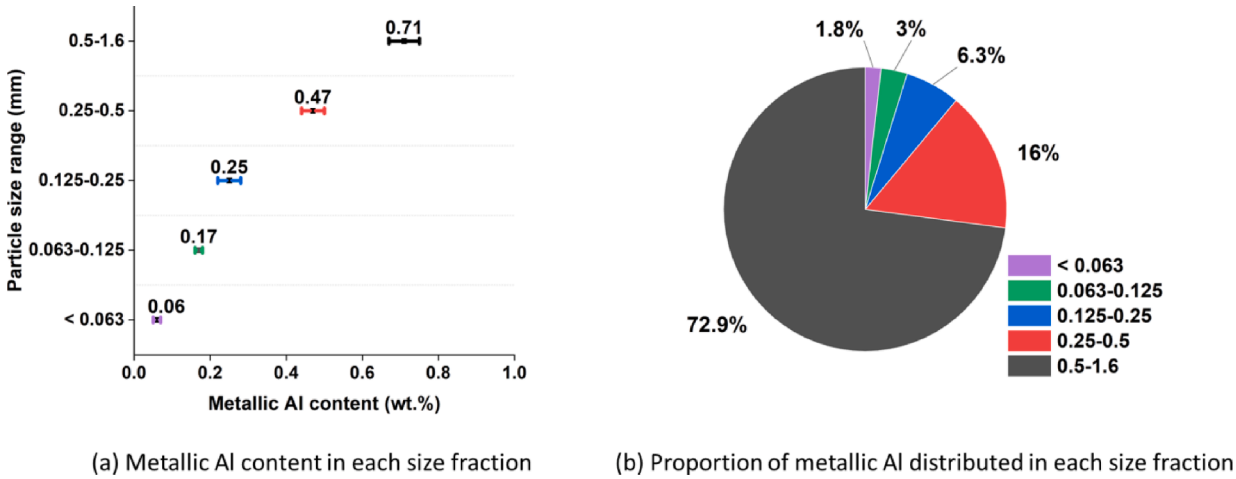

(a) Metallic Al content in each size fraction (b) Proportion of metallic Al distributed in each size fraction

Fig. 3. Comparison among different size fractions of weathered MSWI bottom ash regarding (a) metallic Al content measured by water displacement method; (b) proportion of metallic Al calculated by considering the metallic Al content in each size fraction and the respective weight percentage of that size fraction in weathered MSWI bottom ash.

3.1.2. Weathered MSWI bottom ash particles containing metallic Al

As discussed in Section 3.1.1, the 0.5–1.6 mm size fraction contains the highest percentage of metallic Al in weathered MSWI bottom ash. Therefore, the particles within this size fraction were chosen to investigate the metallic Al embedded in weathered MSWI bottom ash particles. In our preliminary study, a large area phase mapping analysis was performed using SEM-EDS on all weathered MSWI bottom ash particles mounted in the epoxy (see Fig. B3). The analysis results indicated that metallic Al was concentrated in a specific portion of particles, rather than being uniformly distributed in all particles of this size. Fig. 4 provides a representative image of this observation, showing a scan area of 36 mm^2. Among numerous bottom ash particles, only one particle was identified as containing metallic Al (see Fig. 4 (b)). Detailed element maps for Al, O, and Fe can be seen in Fig. C1 (Appendix C).

The weathered MSWI bottom ash particles containing metallic Al exhibit characteristic features. Two typical examples are shown in Fig. 5 (particle 1) and Fig. 6 (particle 2). Fig. 5 (a) and Fig. 6 (a) are backscattered electron (BSE) images. Element maps displaying the distribution of Al, O, Fe, and Mg in these particles are presented in Fig. 5 (b)–(d) and Fig. 6 (b)–(e). The distribution of metallic Al is visualized in Fig. 5 (e) for particle 1 and Fig. 6 (f) for particle 2. In these figures, color coding is applied to identify different phases: dark yellow for metallic Al (Al), blue for oxidized Al (Al-O), and purple for Al-Fe alloy (Al-Fe). The O/Al atomic ratio and elemental composition of each phase are listed in Table C1 (see Appendix C). The following sections provide a detailed analysis of the metallic Al phases and their adjacent phases.

3.1.2.1. Phases classified as metallic Al (Al). The phases in particle 1 show different shades of grey in the BSE image (Fig. 5 (a)). The phases in the areas of bright grey (labeled 1) and light grey (labeled 2) were both classified as metallic Al and colored dark yellow (see Fig. 5 (e)). According to the element maps of O and Al (Fig. 5 (b) and (c)), the concentration of Al in the areas of bright grey and light grey is high, while the concentration of O is almost zero. However, only the area in light grey is composed of 100 % metallic Al. The area in bright grey consists of metallic Al with Fe impurities, as the weak signals of Fe are detected in this area (see Fig. 5 (d)). The metallic Al that contains Fe impurities may come from the aluminum beverage cans in municipal solid waste (Hu et al., 2011).

For particle 2, the phases in the light grey area of the BSE image were categorized as metallic Al (Al) in phase segmentation (see Fig. 6 (a) and (f)). As illustrated in the element maps of O and Al (Fig. 6 (b) and (c)), Al

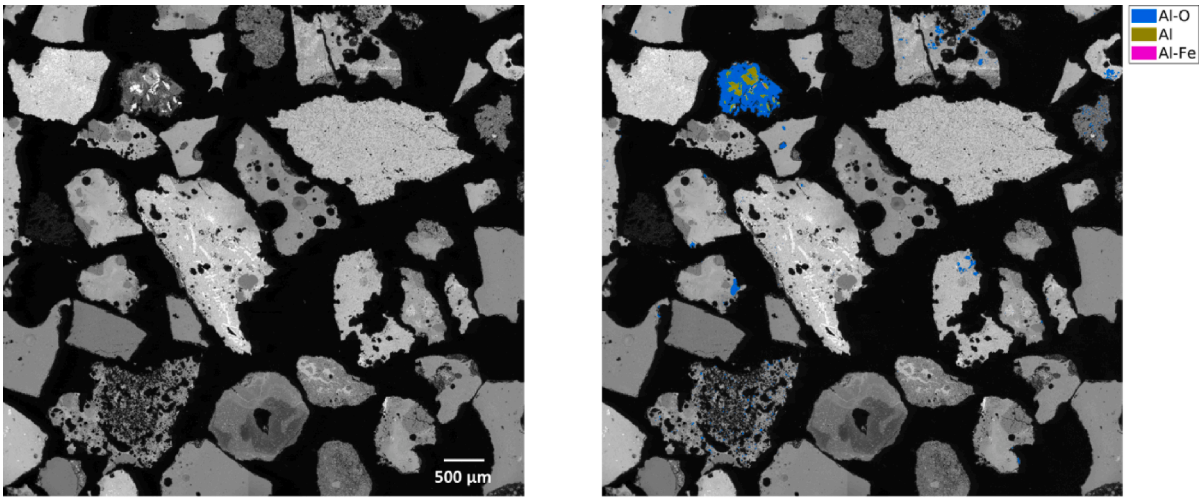

(a) BSE image (b) Image with phase segmentation

Fig. 4. A representative overview of weathered MSWI bottom particles in the 0.5–1.6 mm size fraction, covering an area of 36 mm^2: (a) BSE image; (b) Image obtained after phase segmentation. In this image, labels are as follows: "Al-O" for oxidized Al, "Al" for metallic Al, and "Al-Fe" for Al-Fe alloy.

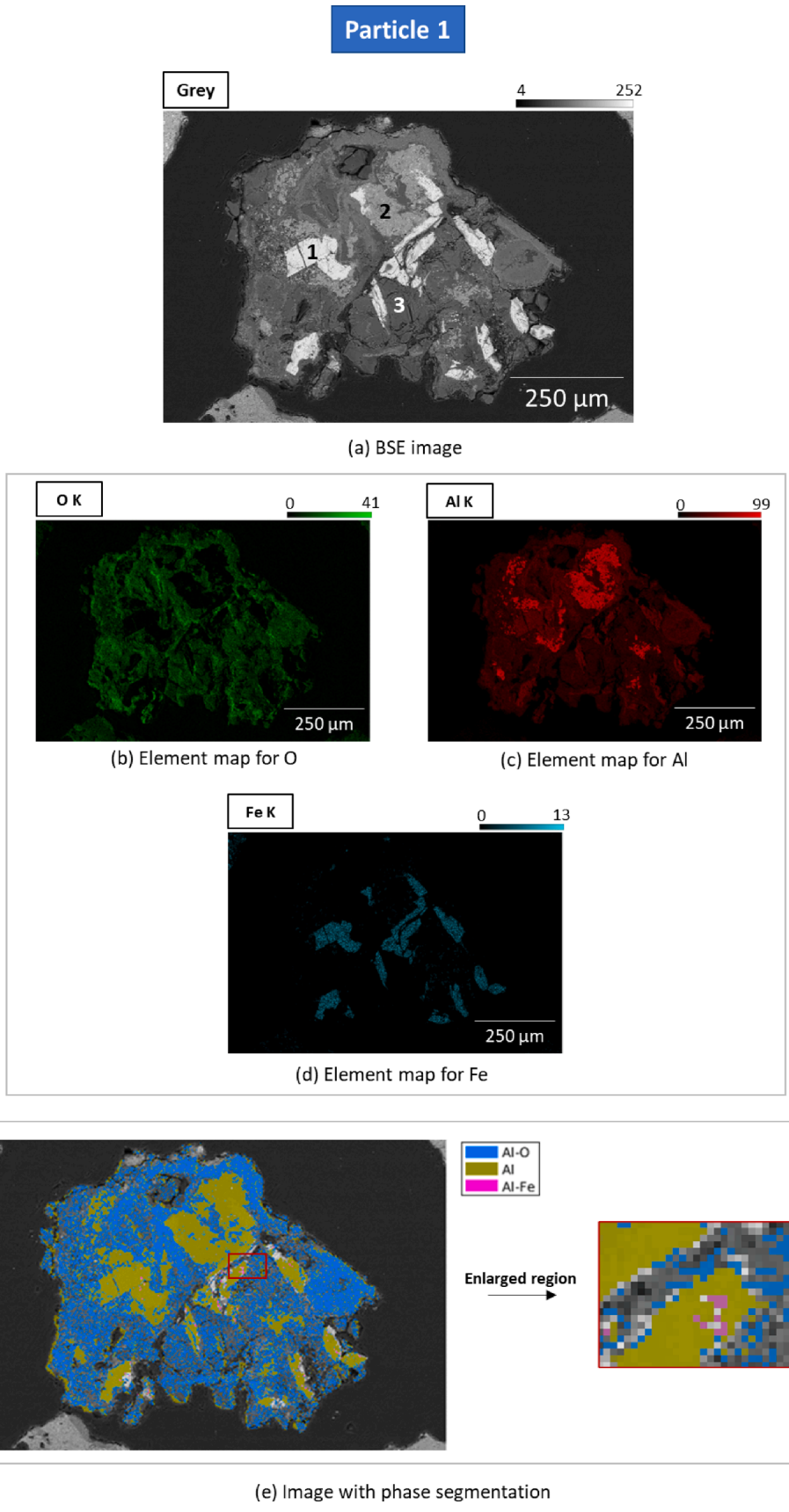

Fig. 5. Typical morphology of weathered MSWI bottom ash particle containing metallic Al (particle 1): (a) BSE image (pixel scan field 512 × 340, area: 0.7 mm^2); (b)–(d) EDS element maps; (e) Image obtained after phase segmentation. In this image, labels are as follows: "Al-O" for oxidized Al, "Al" for metallic Al, and "Al-Fe" for Al-Fe alloy.

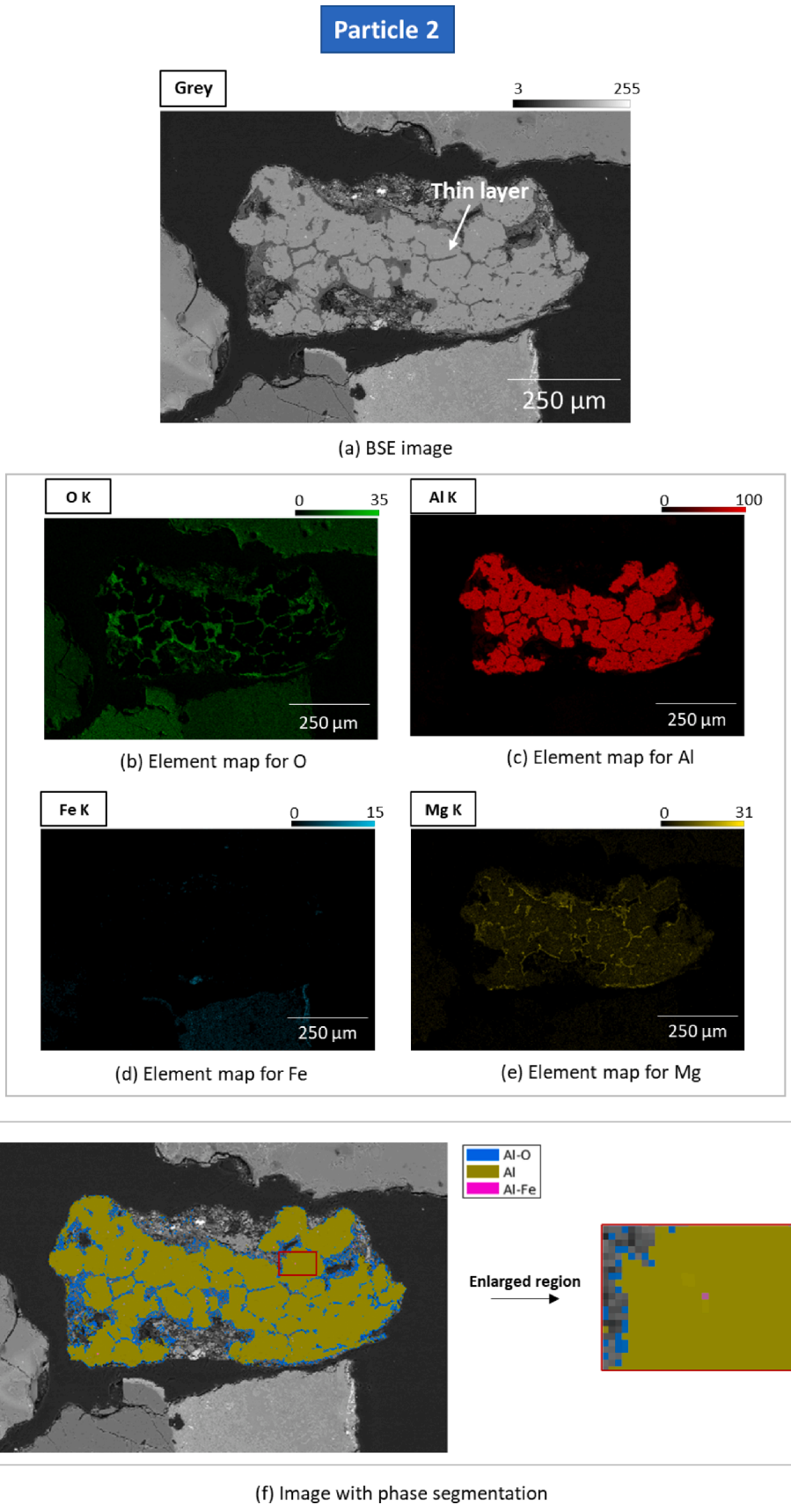

Fig. 6. Typical morphology of weathered MSWI bottom ash particle containing metallic Al (particle 2): (a) BSE image (pixel scan field 512 × 340, area: 0.7 mm^2); (b)–(e) EDS element maps; (f) Image obtained after phase segmentation. In this image, labels are as follows: "Al-O" for oxidized Al, "Al" for metallic Al, and "Al-Fe" for Al-Fe alloy.

is highly concentrated in the light grey area, but the O content is nearly zero. However, the phase in the light grey area of particle 2 is metallic Al with Mg impurities rather than pure metallic Al. The element map of Mg (Fig. 6 (e)) indicates that the phases in this area also incorporate Mg, but the signal of Mg is weak. The metallic Al that contains Mg impurities can be scrunched aluminum-magnesium foil initially used for food packing (Eggen et al., 2020).

Quantitative analysis was performed on the recognized Al phase to validate the results of phase segmentation. As shown in Table C1, the mean value of the O/Al atomic ratio calculated at each pixel is close to zero. This result indicates that the recognized Al phase mainly consists of metallic Al. The Fe/Al ratio is 0.11 for the Al phase in particle 1, and the Mg/Al ratio is 0.03 for the Al phase in particle 2. The low value of these ratios indicates that the content of Fe or Mg is much smaller than that of Al in the recognized Al phase, and these two metals are presented as impurities in metallic Al. It can be concluded that the image analysis used for the separation of metallic Al is reliable.

3.1.2.2. Oxidized Al (Al-O) in the surroundings of metallic Al. The images obtained after phase segmentation (Fig. 5 (e) and Fig. 6 (f)) show that metallic Al is surrounded by oxidized Al (colored blue) in weathered MSWI bottom ash particles. In the phase segmentation, the phases in the areas mainly composed of Al and O were classified as oxidized Al (Al-O). The oxidized Al was found to concentrate in the dark grey area of the BSE image of particle 1 (labeled 3) and particle 2 (thin layers). The average of the O/Al atomic ratio of the pixels in the group of Al-O in particle 1 and particle 2 is 2.9 and 2.8, respectively (Table C1), which are close to the O/Al atomic ratio of $Al(OH)_3$.

Since our weathered MSWI bottom ash particles were ground and polished in a N_2 atmosphere, the oxidation of metallic Al was prevented during the sample preparation process. The oxidized Al detected in weathered MSWI bottom ash could be the oxidation product of aluminum cans, sheets, and foils in household wastes. During the process of metal recycling, MSWI bottom ash particles are usually crushed into small pieces, resulting in the cracking of metallic Al scraps. The exposed surfaces of metallic Al easily react with oxygen and water during the weathering process. The oxidized Al can behave as a protective layer preventing the further oxidation of metallic Al.

The content of oxidized Al indicates the oxidation degree of the metallic Al initially embedded in weathered MSWI bottom ash. In particle 1, the metallic Al was oxidized to a large extent as oxidized Al occupies a large area in the surroundings of metallic Al. The total area percentage of oxidized Al is 35.22 %, larger than the area covered by metallic Al (23.18 %). In comparison, only the surface of the metallic Al was oxidized in particle 2. The oxidized Al layers of 3–15 μm are mainly found along the perimeter of the areas of metallic Al. The metallic Al occupies around 70 % of the area of particle 2, seven times the area of the Al-O phase.

The possible mineralogical composition of the Al-O phase recognized in phase segmentation can be determined with the help of density plots. In the density plots (see Fig. C2 in Appendix C), the location of each point represents the atomic percentages of Al and O at each pixel location in the Al-O phase (Fig. 5 (e) and Fig. 6 (f)). The areas in the density plots were colored according to the number of points located in the area. The area without points was colored dark blue (the relative point density was set at 0). The area with the most densely distributed points was shown in bright yellow (the relative point density was set at 1). In the density plot of particle 1 and particle 2, the bright yellow region lies between the lines representing the O/Al ratio of Al_2O_3 and $Al(OH)_3$. This observation indicates that the Al-O phase in particle 1 and particle 2 could be a mixture of $Al(OH)_3$ and Al_2O_3. This inference is consistent with the results of the XRD analysis that both corundum and gibbsite are present in the bottom ash particles of 0.5–1.6 mm (see Section A.1.2).

3.1.2.3. Al alloy within metallic Al (Al). The phase segmentation results of particle 1 and particle 2 indicate that Al-Fe alloy (colored with purple) is scattered in the areas of metallic Al (Fig. 5 (e) and Fig. 6 (f)). According to the quantitative analysis, the Al-Fe alloy found in weathered MSWI bottom ash particles also contains Si (Table C1). The detection of Al-Fe-Si alloy in MSWI bottom ash particles was also reported by Saffarzadeh et al. (Saffarzadeh et al., 2016). The formation of Al alloy can be induced by the melting of metallic Al during waste incineration. The melting point of pure metallic Al is around 660 °C (Davis, 1999), lower than the temperature in the waste incinerator (between 700 and 1100 °C) (Bunge, 2016). The metallic Al scraps of small size or the surface of large metallic Al scraps will melt during the waste incineration process. The formation of the liquidus metallic Al could lead to the adherence of the minerals on the surface of metallic Al scraps, as observed in particle 2 (Fig. 6 (f)). The presence of Fe and Si could reduce the temperature when metallic Al becomes liquid, resulting in the formation of Al-Fe-Si alloy (Saffarzadeh et al., 2016).

3.2. Mechanical removal of metallic Al from weathered MSWI bottom ash

Considering the distribution of metallic Al in weathered MSWI bottom ash, the mechanical treatments are more suitable than chemical treatments and thermal treatments for the reduction of metallic Al content. As presented in Section 3.1, around 90 % of the metallic Al detected in weathered MSWI bottom ash are embedded in particles larger than 0.25 mm. The metallic Al in these particles is surrounded by oxidized Al (a mixture of Al_2O_3 and $Al(OH)_3$), which usually functions as a protective layer and prevents the oxidation of metallic Al. The oxidation rate of metallic Al can be slow during chemical treatments and thermal treatments. It is worth noting that the efficiency of chemical treatments and thermal treatments on the oxidation of metallic Al can be improved after the mechanical treatments of weathered MSWI bottom ash (Bertolini et al., 2004; Xuan and Poon, 2018). This is because the grinding of weathered MSWI bottom ash can break the oxidized Al layers on the surface of metallic Al. Therefore, mechanical treatments may offer significant advantages in practical waste management scenarios.

3.2.1. Effectiveness of mechanical treatments on metallic Al removal from weathered MSWI bottom ash

Fig. 7 (a) depicts the mechanical treatments of weathered MSWI bottom ash at optimal milling speed and duration. In the milling process, the brittle minerals were broken into small fragments while ductile metals were pressed into plate-shaped scraps. The images of separated metal scraps and MBA are shown in Fig. 7 (a). The plate-shaped metal scraps separated from GBA have a diameter of up to 1 mm, much larger than the particle size of MBA. The size difference between MBA and metal scraps enables their separation by sieving.

Mechanical treatments reduced the metallic Al content in weathered MSWI bottom ash from an initial 0.56 wt% to 0.13 wt%. The metallic Al content in MBA (0.13 wt%) is close to that in the ground MSWI bottom ash used by Tang et al. (Tang et al., 2016), Caprai (Caprai, 2019), and Alderete et al. (Alderete et al., 2021) for the application as SCM. Mechanical treatments significantly reduced the metallic Al content in weathered MSWI bottom ash by 77 %. Given that the metallic Al found in the 0.5–1.6 mm particle size fraction constitutes 72.9 % of the total weight of the metallic Al in weathered MSWI bottom ash, it can be concluded that most of the metallic Al removed by the mechanical treatments came from this size fraction.

The effects of mechanical treatments on large and small particles of weathered MSWI bottom ash are different. During the milling process, the metallic Al embedded in the MSWI bottom ash particles of 0.5–1.6 mm is more likely to be pressed into plate-shaped scraps. This is because metallic Al can occupy up to 70 % of the area in the MSWI bottom ash particle (see Section 3.1.2.2). Weathered MSWI bottom ash mainly consists of mineral phases, while metals are only present in trace amounts. As illustrated in Fig. 7 (b), metals can be separated from

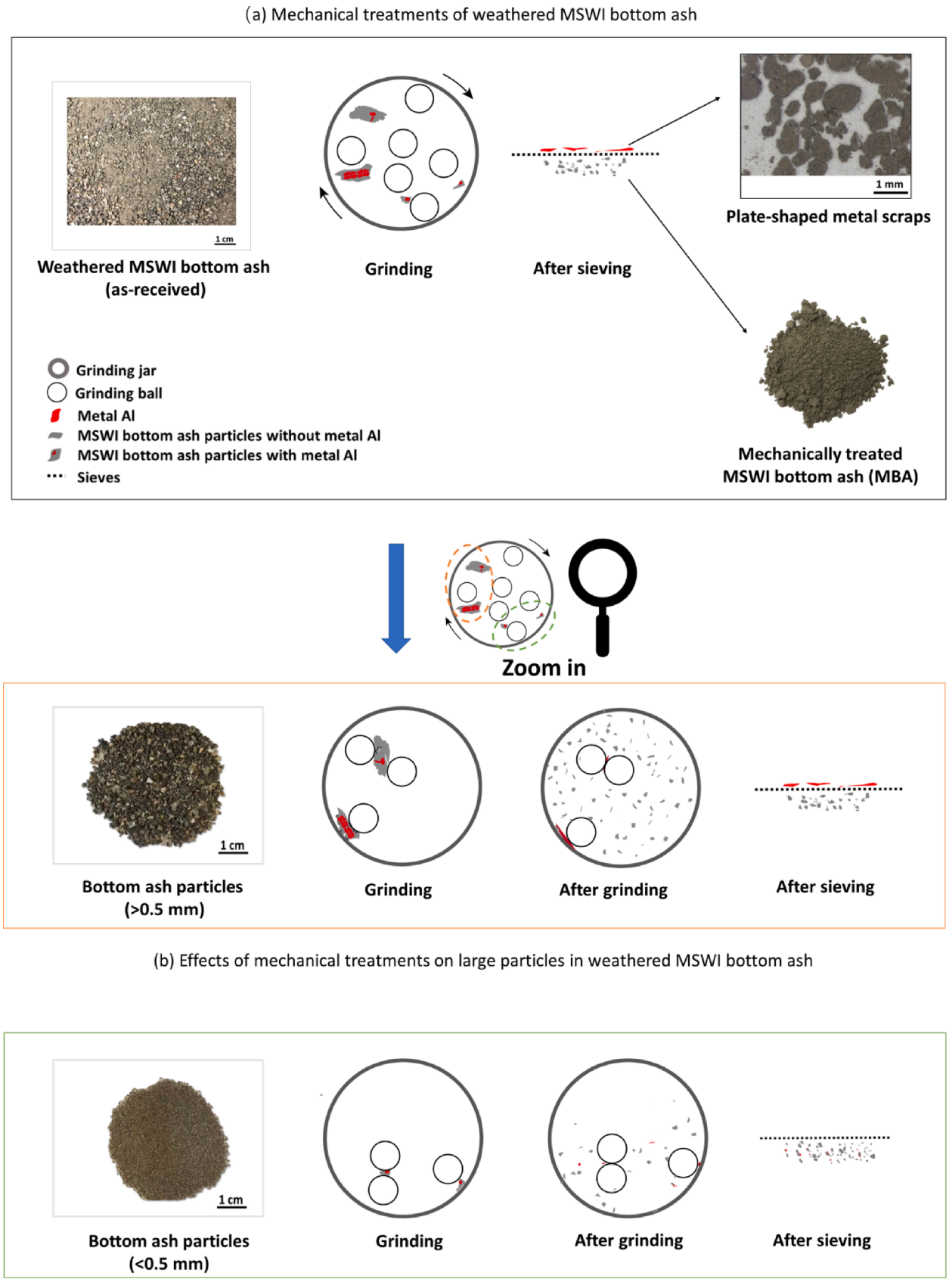

Fig. 7. Illustration of the mechanical removal process of metallic Al: (a) mechanical treatments of weathered MSWI bottom ash particles (mix of all size fractions); (b) effects of grinding and sieving on large MSWI bottom ash particles (>0.5 mm); (c) effects of grinding and sieving on small MSWI bottom ash particles (<0.5 mm).

ground MSWI bottom ash by sieving when the size of metal plate-shaped scraps is larger than the mineral particles.

Compared with metallic Al in the particles of 0.5–1.6 mm, the size of metallic Al embedded in weathered MSWI bottom ash with particle size smaller than 0.5 mm is also smaller. After grinding, these metallic Al scraps easily fall in the same size range as the minerals derived from the pulverization of weathered MSWI bottom ash in 0.5–1.6 mm size fraction. As shown in Fig. 7 (c), the separation of metallic Al from GBA is difficult when it has a particle size similar to that of the mineral particles. From this perspective, most of the residual metallic Al detected in MBA is originally embedded in weathered MSWI bottom ash particles smaller than 0.5 mm.

3.2.2. *Effects of mechanical treatments on the composition of weathered MSWI bottom ash*

The GBA was produced after grinding weathered MSWI bottom ash, while the MBA was obtained after sieving the GBA to remove metal scraps (see Fig. 7). The XRD patterns of GBA and MBA are almost the same (see Fig. D1), indicating that these two have nearly the same mineralogical composition. The main difference between GBA and MBA lies in the peaks of metallic Al. The metallic Al peak at 2θ of 38.5° in the spectrum of GBA is not observed in the XRD spectrum of MBA. This change is mainly caused by the decrease in the metallic Al content.

The metallic Al content in sieved metal scraps is only around 27.8 wt %, as determined by the water displacement method. In addition to metallic Al, other metals were also separated from weathered MSWI bottom ash during mechanical treatments. As shown in Fig. D1, separated metal scraps consist of aluminum (Al, ICSD 251015), khatyrkite (Al_2Cu, ICSD 42517), copper (Cu, ICSD 261638), and iron (Fe, ICSD 1503158). In the XRD spectrum of metal scraps, peaks of quartz (SiO_2, ICSD 541929) and magnetite (Fe_2O_3, ICSD 92356), albeit with low intensity, are also observed.

3.2.3. *Effectiveness of mechanical treatments in improving compressive strength of blended cement pastes prepared with weathered MSWI bottom ash*

As shown in Fig. 8 (a), at the replacement level of 25 wt%, voids, cracks, and volume expansion are observed in the sample of GBA-CEM. These issues arise from the release of hydrogen gas after the redox reaction of metallic Al present in GBA. Comparatively, blended cement paste samples made from 25 wt% MBA do not show apparent defects (Fig. 8 (b)). This can be ascribed to the significantly lower content of metallic Al in MBA compared to GBA. The 28-day compressive strength of MBA-CEM is two times as high as that of GBA-CEM (see Fig. 8 (c)), indicating that the adverse effects of metallic Al on strength developments can be effectively mitigated after the mechanical treatments of weathered MSWI bottom ash. When comparing FA-CEM and GBA-CEM, the compressive strength of GBA-CEM is close to that of FA-CEM. This test result shows that weathered MSWI bottom ash, after reducing its metallic Al content via mechanical treatments, has the potential to be used as an alternative to Class F coal fly ash.

4. Conclusions

In this study, the distribution of metallic aluminum (Al) in weathered municipal solid waste incineration (MSWI) bottom ash was thoroughly characterized. Based on the characterization results, mechanical treatments (consisting of grinding and sieving) were chosen to reduce the

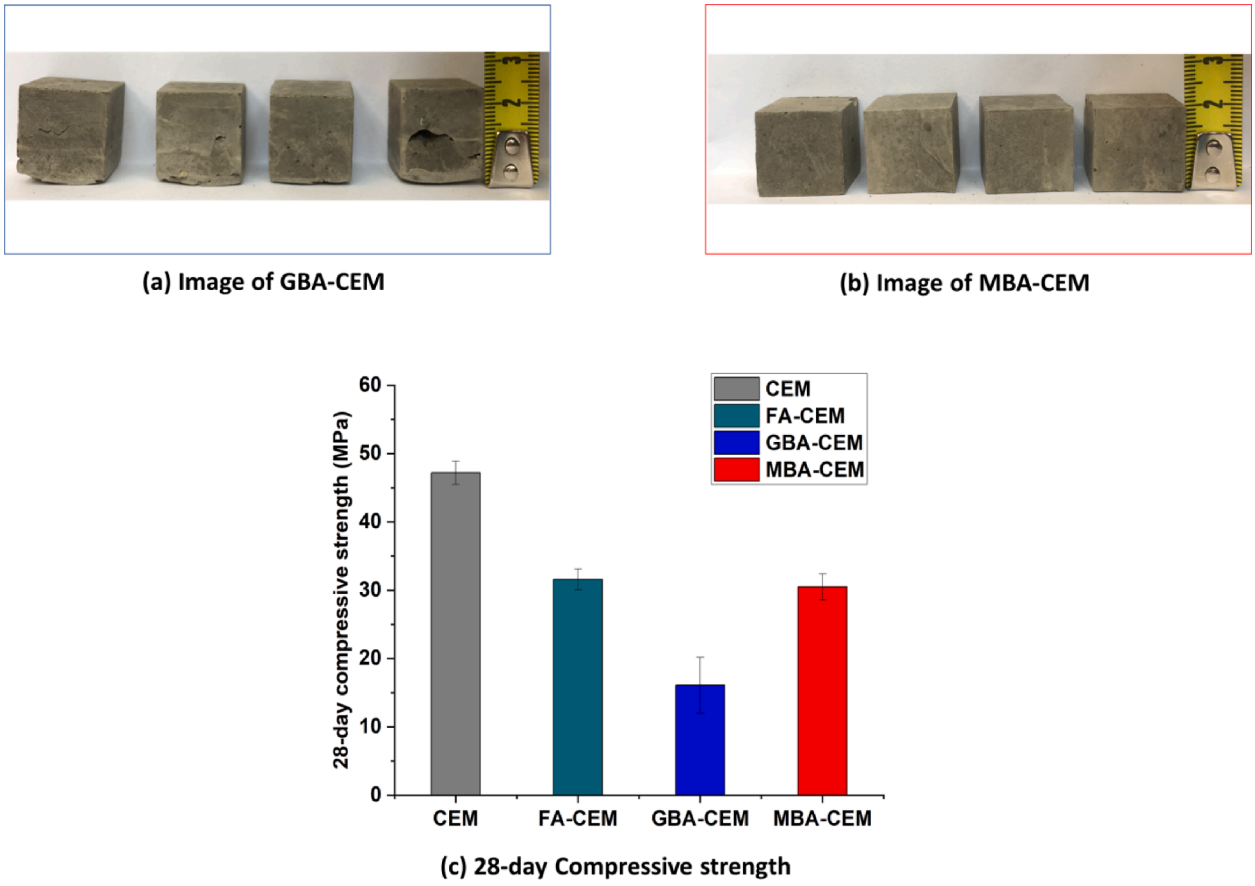

Fig. 8. (a) Blended cement paste samples prepared with ground weathered MSWI bottom ash (GBA-CEM); (b) Blended cement paste samples prepared with mechanical-treated weathered MSWI bottom ash (MBA-CEM); (c) 28-day compressive strength of plain cement (CEM) and blended cement paste samples. FA-CEM is blended cement paste prepared using class F coal fly ash as SCM.

metallic Al content in weathered MSWI bottom ash. The effectiveness and limitations of mechanical treatments in removing metallic Al from weathered MSWI bottom ash were discussed. The following conclusions can be drawn:

Around 73 % of the metallic Al in weathered MSWI bottom ash was found in the 0.5–1.6 mm size fraction. Nonetheless, metallic Al was not uniformly distributed across all particles of this size but concentrated in specific portions. The weathered MSWI bottom ash particles containing metallic Al have two typical morphologies. The main differences between these two types of particles are the thickness of the oxidized Al layers on the surface of metallic Al and the area percentage of metallic Al in the particle. The oxidized Al layers consist of Al_2O_3 and $Al(OH)_3$.

After mechanical treatments, metallic Al content was reduced by 77 %, and the particle size was reduced to below 63 μm. Most metallic Al removed by mechanical treatments is from 0.5 to 1.6 mm weathered MSWI bottom ash particles. The metallic Al embedded in smaller weathered MSWI bottom ash particles is difficult to be removed by mechanical treatments. The key to removing metallic Al by sieving lies in creating a size difference between metal scraps and mineral components of weathered MSWI bottom ash during the milling process.

The volume expansion and strength reduction caused by replacing cement with weathered MSWI bottom ash could be mitigated after reducing the metallic Al content in weathered MSWI bottom ash. The mechanically treated MSWI bottom ash (MBA) with metallic Al content of 0.13 wt% has the potential to be used as an alternative to Class F coal fly ash to prepare blended cement pastes. At a replacement level of 25 wt % and a water-to-binder ratio of 0.5, the 28-day compressive strength of blended cement paste prepared with MBA is similar to that prepared using Class F coal fly ash.

The metal scraps are the by-products of the mechanical treatments of weathered MSWI bottom ash and contain only around 27.8 wt% metallic Al. The metal scraps also contain other types of metals and traces of minerals. Considering the low purity and low yield of these metal scraps, metal recovery may require significant efforts.

CRediT authorship contribution statement

Boyu Chen: Conceptualization, Data curation, Formal analysis, Investigation, Methodology, Writing – original draft, Writing – review & editing. **Jiayi Chen:** Data curation, Software, Writing – review & editing. **Fernando França de Mendonça Filho:** Investigation, Writing – review & editing. **Yubo Sun:** Investigation, Writing – review & editing. **Marc Brito van Zijl:** Resources, Writing – review & editing. **Oguzhan Copuroglu:** Investigation, Writing – review & editing. **Guang Ye:** Supervision, Writing – review & editing.

Declaration of competing interest

The authors declare that they have no known competing financial interests or personal relationships that could have appeared to influence the work reported in this paper.

Data availability

Data will be made available on request.

Acknowledgements

Boyu Chen would like to thank the Chinese Scholarship Council for their support for her Ph.D. study. Financial support by Mineralz (Part of Renewi) is acknowledged. Special acknowledgment is given to Professor Klaas van Breugel for his help with the improvement of text writing. Dr. Nicola Döbelin from RMS Foundation is gratefully acknowledged for the QXRD analysis. Ruud Hendrix at the Department of Materials Science and Engineering of the Delft University of Technology is acknowledged for the X-ray analysis. Arjan Thijssen, Ton Blom, Maiko van Leeuwen, and John van de Berg, from the Stevin lab and Microlab at the Faculty of Civil Engineering and Geosciences, Delft University of Technology, are acknowledged for their support for all the experiments.

Appendix A. Supplementary material

Supplementary data to this article can be found online at https://doi.org/10.1016/j.wasman.2024.01.031.

References

Alderete, N.M., Joseph, A.M., Van den Heede, P., Matthys, S., De Belie, N., 2021. Effective and sustainable use of municipal solid waste incineration bottom ash in concrete regarding strength and durability. Resour. Conserv. Recycl. 167 https://doi.org/10.1016/j.resconrec.2020.105356.

Bertolini, L., Carsana, M., Cassago, D., Curzio, A.Q., Collepardi, M., 2004. MSWI ashes as mineral additions in concrete. Cem. Concr. Res. 34, 1899–1906. https://doi.org/10.1016/j.cemconres.2004.02.001.

Bunge, R., 2016. Recovery of metals from waste incinerator bottom ash [WWW Document]. URL https://vbsa.ch/wp-content/uploads/2016/07/Studie-Bunge-Internetversion.pdf.

Caprai, V., 2019. Treatment and Valorization of Municipal Solid Waste Incineration Bottom Ash. Eindhoven University of Technology.

Carsana, M., Gastaldi, M., Lollini, F., Redaelli, E., Bertolini, L., 2016. Improving durability of reinforced concrete structures by recycling wet-ground MSWI bottom ash. Mater. Corros. 67, 573–582. https://doi.org/10.1002/maco.201608881.

Chen, B., 2023. Utilization of mswi bottom ash as a mineral resource for low-carbon construction materials: quality-upgrade treatments. Mix Design Method, and Microstructure Analysis. Delft University of Technology.

Chen, B., van Zijl, M.B., Keulen, A., Ye, G., 2020. Thermal Treatment on MSWI Bottom Ash for the Utilisation in Alkali Activated Materials. KnE Eng. doi: 10.18502/keg.v5i4.6792.

Chen, B., Perumal, P., Illikainen, M., Ye, G., 2023a. A review on the utilization of municipal solid waste incineration (MSWI) bottom ash as a mineral resource for construction materials. J. Build. Eng. 106386. doi: 10.1016/j.jobe.2023.106386.

Chen, B., Sun, Y., Jacquemin, L., Zhang, S., Blom, K., Luković, M., Ye, G., 2019. Pre-treatments of MSWI bottom ash for the application as supplementary cementitious material in blended cement paste. In: Proceedings of the International Conference on Sustainable Materials, Systems and Structures. RILEM Publications, pp. 187–193.

Chen, B., Zuo, Y., Zhang, S., de Lima Junior, L.M., Liang, X., Chen, Y., van Zijl, M.B., Ye, G., 2023b. Reactivity and leaching potential of municipal solid waste incineration (MSWI) bottom ash as supplementary cementitious material and precursor for alkali-activated materials. Constr. Build. Mater. 409, 133890 https://doi.org/10.1016/j.conbuildmat.2023.133890.

Chimenos, J.M., Segarra, M., Fernandez, M.A., Espiell, F., 1999. Characterization of the bottom ash in municipal solid waste incinerator. J. Hazard. Mater. A.

Chimenos, J.M., Fernández, A.I., Nadal, R., Espiell, F., 2000. Short-term natural weathering of MSWI bottom ash. J. Hazard. Mater. 79, 287–299. 10.1016/S0304-3894(00)00270-3.

Davis, J.R., 1999. Corrosion of Aluminum and Aluminum Alloys. ASM International.

de Vries, W., 2017. ADR: The Use of Advanced Dry Recovery in Recycling Fine Moist Granular Materials. Delft University of Technology.

de Vries, W., Rem, P., Berkhout, P., 2009. ADR: A new method for dry classification. In: Proceedings of the ISWA International Conference. pp. 12, 103–113.

Eggen, S., Sandaunet, K., Kolbeinsen, L., Kvithyld, A., 2020. Recycling of aluminium from mixed household waste. Miner. Met. Mater. Ser. 1091–1100. https://doi.org/10.1007/978-3-030-36408-3_148.

Eurostat (Statistical Office of the European Communities), 2023. Municipal waste statistics [WWW Document]. URL https://ec.europa.eu/eurostat/statistics-explained/index.php?title=Municipal_waste_statistics#Municipal_waste_generation.

Grand View Research, 2019. Waste To Energy Market Size | Industry Report, 2020-2027 [WWW Document]. URL https://www.grandviewresearch.com/industry-analysis/waste-to-energy-technology-industry.

Holm, O., Simon, F.G., 2017. Innovative treatment trains of bottom ash (BA) from municipal solid waste incineration (MSWI) in Germany. Waste Manag. 59, 229–236. https://doi.org/10.1016/j.wasman.2016.09.004.

Hu, Y., Bakker, M.C.M., de Heij, P.G., 2011. Recovery and distribution of incinerated aluminum packaging waste. Waste Manag. 31, 2422–2430. https://doi.org/10.1016/j.wasman.2011.07.021.

International Energy Agency (IEA), 2009. Cement Technology Roadmap: Carbon Emissions Reductions up to 2050 [WWW Document]. URL https://www.iea.org/reports/cement-technology-roadmap-carbon-emissions-reductions-up-to-2050.

International Renewable Energy Agency (IRENA), 2022. Renewable Capacity Statistics 2022 [WWW Document]. URL https://www.irena.org/-/media/Files/IRENA/Agency/Publication/2022/Apr/IRENA_RE_Capacity_Statistics_2022.pdf?rev=460f190dea15442eba8373d9625341ae.

Joseph, A.M., Snellings, R., Nielsen, P., Matthys, S., Belie, N.D., 2020. Pre-treatment and utilisation of municipal solid waste incineration bottom ashes towards a circular economy. Constr. Build. Mater. 260, 120485 https://doi.org/10.1016/j.conbuildmat.2020.120485.

Keulen, A., Zomeren, A.V., Harpe, P., Aarnink, W., Simons, H.A.E., Brouwers, H.J.H., 2016. High performance of treated and washed MSWI bottom ash granulates as

natural aggregate replacement within earth-moist concrete. Waste Manag. 49, 83–95. https://doi.org/10.1016/j.wasman.2016.01.010.
Kim, J., An, J., Nam, B.H., Tasneem, K.M., 2016. Investigation on the side effects of municipal solid waste incineration ashes when used as mineral addition in cement-based material. Road Mater. Pavement Des. 17, 345–364. https://doi.org/10.1080/14680629.2015.1083463.
Li, X.G., Lv, Y., Ma, B.G., Chen, Q.B., Yin, X.B., Jian, S.W., 2012. Utilization of municipal solid waste incineration bottom ash in blended cement. J. Clean. Prod. 32, 96–100. https://doi.org/10.1016/j.jclepro.2012.03.038.
Lin, K.L., Chang, W.C., Lin, D.F., 2008. Pozzolanic characteristics of pulverized incinerator bottom ash slag. Constr. Build. Mater. 22, 324–329. https://doi.org/10.1016/j.conbuildmat.2006.08.012.
Lin, K.L., Lin, D.F., 2006. Hydration characteristics of municipal solid waste incinerator bottom ash slag as a pozzolanic material for use in cement. Cem. Concr. Compos. 28, 817–823. https://doi.org/10.1016/j.cemconcomp.2006.03.003.
Liu, Y., Sidhu, K.S., Chen, Z., Yang, E.H., 2018. Alkali-treated incineration bottom ash as supplementary cementitious materials. Constr. Build. Mater. 179, 371–378. https://doi.org/10.1016/j.conbuildmat.2018.05.231.
Lo, F.C., Lo, S.L., Lee, M.G., 2020. Effect of partially replacing ordinary Portland cement with municipal solid waste incinerator ashes and rice husk ashes on pervious concrete quality. Environ. Sci. Pollut. Res. 27, 23742–23760. https://doi.org/10.1007/S11356-020-08796-Z.
Loginova, E., Schollbach, K., Proskurnin, M., Brouwers, H.J.H., 2021. Municipal solid waste incineration bottom ash fines: transformation into a minor additional constituent for cements. Resour. Conserv. Recycl. 166 https://doi.org/10.1016/j.resconrec.2020.105354.
Margallo, M., Aldaco, R., Irabien, Á., 2014. Environmental management of bottom ash from municipal solid waste incineration based on a life cycle assessment approach. Clean Technol. Environ. Policy, 167(16), 1319–1328. doi: 10.1007/S10098-014-0761-4.
Muchova, L., Bakker, E., Rem, P., 2009. Precious metals in municipal solid waste incineration bottom ash. Water Air Soil Pollut. Focus 9, 107–116. https://doi.org/10.1007/s11267-008-9191-9.
National Bureau of Statistics of China (NBS), 2022. Urban Garbage Collection and Disposal Situation [WWW Document]. URL https://data.stats.gov.cn/easyquery.htm?cn=E0103.
NEN-EN 196-1, 2016. Methods of testing cement - Part 1: Determination of strength [WWW Document]. URL https://connect.nen.nl/Standard/Detail/219352?compId=10037&collectionId=0.
NEN-EN 933-1, 2012. Tests for geometrical properties of aggregates - Part 1: Determination of particle size distribution - Sieving method [WWW Document]. URL https://connect.nen.nl/Standard/Detail/167446?compId=10037&collectionId=0.
NEN-EN 933-2, 2020. Tests for geometrical properties of aggregates - Part 2: Determination of particle size distribution - Test sieves, nominal size of apertures [WWW Document]. URL https://connect.nen.nl/Standard/Detail/3633404?compId=10037&collectionId=0.
Neuwahl, F., Cusano, G., Benavides, J.G., Holbrook, S., Roudier, S., 2019. Best Available Techniques (BAT) Reference Document for Waste Incineration. Publications Office of the European Union. doi: 10.2760/761437.
Otsu, N., 1979. A threshold selection method from gray-level histograms. IEEE Trans. Syst. Man Cybern. 9, 62–66. https://doi.org/10.1109/TSMC.1979.4310076.
Qiao, X.C., Ng, B.R., Tyrer, M., Poon, C.S., Cheeseman, C.R., 2008. Production of lightweight concrete using incinerator bottom ash. Constr. Build. Mater. 22, 473–480. https://doi.org/10.1016/j.conbuildmat.2006.11.013.
Rem, P.C., Vries, C.D., Kooy, L.A.V., Bevilacqua, P., Reuter, M.A., 2004. The Amsterdam pilot on bottom ash. Miner. Eng. 363–365. https://doi.org/10.1016/j.mineng.2003.11.009.
Saffarzadeh, A., Shimaoka, T., Wei, Y., Gardner, K.H., Musselman, C.N., 2011. Impacts of natural weathering on the transformation/neoformation processes in landfilled MSWI bottom ash: a geoenvironmental perspective. Waste Manag. 31, 2440–2454. https://doi.org/10.1016/j.wasman.2011.07.017.
Saffarzadeh, A., Arumugam, N., Shimaoka, T., 2016. Aluminum and aluminum alloys in municipal solid waste incineration (MSWI) bottom ash: a potential source for the production of hydrogen gas. Int. J. Hydrogen Energy 41, 820–831. https://doi.org/10.1016/j.ijhydene.2015.11.059.
Simões, B., da Silva, P.R., Silva, R.V., Avila, Y., Forero, J.A., 2021. Ternary mixes of self-compacting concrete with fly ash and municipal solid waste incinerator bottom ash. Appl. Sci. 11, 1–17. https://doi.org/10.3390/app11010107.
Speiser, C., Baumann, T., Niessner, R., 2000. Morphological and chemical characterization of calcium-hydrate phases formed in alteration processes of deposited municipal solid waste incinerator bottom ash. Environ. Sci. Technol. 34, 5030–5037. https://doi.org/10.1021/es990739c.
Sun, Y., Chen, B., Zhang, S., Blom, K., Luković, M., Ye, G., 2019. Investigation on the potential application of MSWI bottom ash as cement substitutes. In: Proceedings of Slag Valorisation Symposium.
Šyc, M., Simon, F.G., Hykš, J., Braga, R., Biganzoli, L., Costa, G., Funari, V., Grosso, M., 2020. Metal recovery from incineration bottom ash: state-of-the-art and recent developments. J. Hazard. Mater. 393, 122433 https://doi.org/10.1016/j.jhazmat.2020.122433.
Tang, P., Florea, M.V.A., Spiesz, P., Brouwers, H.J.H., 2016. Application of thermally activated municipal solid waste incineration (MSWI) bottom ash fines as binder substitute. Cem. Concr. Compos. 70, 194–205. https://doi.org/10.1016/j.cemconcomp.2016.03.015.
United States Environmental Protection Agency (US EPA), 2022. National Overview: Facts and Figures on Materials, Wastes and Recycling [WWW Document]. URL https://www.epa.gov/facts-and-figures-about-materials-waste-and-recycling/national-overview-facts-and-figures-materials.
van de Wouw, P.M.F., Loginova, E., Florea, M.V.A., Brouwers, H.J.H., 2020. Compositional modelling and crushing behaviour of MSWI bottom ash material classes. Waste Manag. 101, 268–282. https://doi.org/10.1016/j.wasman.2019.10.013.
Xuan, D., Poon, C.S., 2018. Removal of metallic Al and Al/Zn alloys in MSWI bottom ash by alkaline treatment. J. Hazard. Mater. 344, 73–80. https://doi.org/10.1016/j.jhazmat.2017.10.002.
Yang, Z., Ji, R., Liu, L., Wang, X., Zhang, Z., 2018a. Recycling of municipal solid waste incineration by-product for cement composites preparation. Constr. Build. Mater. 162, 794–801. https://doi.org/10.1016/j.conbuildmat.2017.12.081.
Yang, Z., Tian, S., Liu, L., Wang, X., Zhang, Z., 2018b. Recycling ground MSWI bottom ash in cement composites: long-term environmental impacts. Waste Manag. 78, 841–848. https://doi.org/10.1016/j.wasman.2018.07.002.
Yao, Z.T., Ji, X.S., Sarker, P.K., Tang, J.H., Ge, L.Q., Xia, M.S., Xi, Y.Q., 2015. A comprehensive review on the applications of coal fly ash. Earth-Sci. Rev. 141, 105–121. 10.1016/j.earscirev.2014.11.016.